HHS Public Access

Author manuscript

Cell. Author manuscript; available in PMC 2016 June 04.

Published in final edited form as:

Cell. 2015 June 4; 161(6): 1280–1292. doi:10.1016/j.cell.2015.05.007.

Structural repertoire of HIV-1-neutralizing antibodies targeting the CD4 supersite in 14 donors

A full list of authors and affiliations appears at the end of the article.

Abstract

The site on the HIV-1 gp120 glycoprotein that binds the CD4 receptor is recognized by broadly reactive antibodies, several of which neutralize over 90% of HIV-1 strains. To understand how antibodies achieve such neutralization, we isolated CD4-binding-site (CD4bs) antibodies and analyzed 16 co-crystal structures –8 determined here– of CD4bs antibodies from 14 donors. The 16 antibodies segregated by recognition mode and developmental ontogeny into two types: CDR H3-dominated and V_H-gene-restricted. Both could achieve greater than 80% neutralization breadth, and both could develop in the same donor. Although paratope chemistries differed, all 16 gp120-CD4bs antibody complexes showed geometric similarity, with antibody-neutralization breadth correlating with antibody-angle of approach relative to the most effective antibody of each type. The repertoire for effective recognition of the CD4 supersite thus comprises antibodies with distinct paratopes arrayed about two optimal geometric orientations, one achieved by CDR H3 ontogenies and the other achieved by V_H-gene-restricted ontogenies.

[#]To whom correspondence should be addressed: jmascola@nih.gov (J.R.M.) and pdkwong@nih.gov (P.D.K.).
[*]Equal contribution.

AUTHOR CONTRIBUTIONS

T.Z., R.M.L, L.C., P.A., L.Sh., J.R.M. and P.D.K. designed research, analyzed data, and assembled and wrote the paper, on which all principal investigators commented. R.M.L., X.W. and N.A.D. isolated and characterized VRC13, VRC16, VRC18 and VRC27 antibodies with assistance from M.J.E., L.T., and Z.Y., and with R.T.B, M.K.L., K.M., S.O. and S.D.S. performing neutralization assays. T.Z., L.C. and P.A. led the structure determination and analysis with assistance from T.S.L, S.M., S.S. and A.Z, and with A.D., Y.Y. and B.Z. expressing HIV-1 gp120 cores and antibodies for crystallization and binding and T.Z. and M.P. performing trimer modeling. L.C., M.G.J., M.D.G. and L.St. produced germline antibodies and assessed binding to HIV-1 gp120. R.M.L. and X.W. prepared samples for 454 pyrosequencing; NISC and J.C.M performed next-generation sequencing; C.S., L.Sh. and P.D.K. carried out bioinformatics. N.S.L. contributed to repertoire analysis, and A.P.W. and P.J.B. contributed to ontogeny analysis. I.S.G. performed neutralization fingerprinting, and T.K. and I.S.G. defined the CD4 supersite by antibody potency. T.G., H.-P.P., A.-S.Y. and L.Sh. analyzed antibody paratope chemistry. D.L. and R.K. performed B cell activation experiments. R.M.L. analyzed donor sera potency and breadth with D.R.B., W.C.K., M.S.C., B.F.H., J.P.C., M.C., J.F.S. and M.C.N. contributing donor samples. D.C., A.L, Q.J.S. and R.A.W provided antibody HJ16; J.F.S. and M.C.N. provided antibodies 1B2530, 8ANC131 and 8ANC134.

ACCESSION NUMBERS

Coordinates and structure factors for the CD4-binding site antibodies in complex with HIV-1 gp120 have been deposited with the Protein Data Bank under accession codes: 4YDJ, 4YDK, 4YDL, 4YDI, 4RWY, 4RX4, 4YFL and 4YE4. Nucleotide sequences for heavy chain variable regions of antibodies 44-VRC13.01, 44-VRC13.02, C38-VRC16.01, C38-VRC16.02 and C38-VRC18.02 have been deposited under Genbank accession numbers KP860914 through KP860918. Next-generation sequencing data for donors 44, C38 (for VRC16.01), RU01 and RU08 have been deposited with the National Center for Biotechnology Information Short Reads Archives (SRA) under accession code SRP055520.

SUPPLEMENTAL INFORMATION

Supplemental Information includes Extended Experimental Procedures, seven figures, and seven tables and can be found with this article online at http://dx.doi.org/xxx.

INTRODUCTION

Successful vaccines often recapitulate effective immune responses induced by natural infection. In the case of HIV-1, antibodies capable of neutralizing about half of circulating strains develop after years of chronic infection in about half of examined donors (Hraber et al., 2014). Isolation and mapping of these neutralizing responses show that they target most of the exposed surface of the prefusion mature closed state of the HIV-1 Env spike (Julien et al., 2013; Lyumkis et al., 2013; Pancera et al., 2014). Despite this broad targeting, highly effective antibodies develop preferentially against just a few sites of vulnerability on HIV-1 Env. These "supersites" of vulnerability have been the focus of intense vaccine interest. Each supersite appears to be targeted by broadly neutralizing antibodies that arise in many infected individuals, by broadly neutralizing antibodies with diverse modes of recognition, and by broadly neutralizing antibodies with diverse B cell ontogenies (reviewed in (Kwong and Mascola, 2012; West et al., 2014)). Thus the human immune system has multiple avenues by which to generate effective antibodies against these supersites, thereby providing a rationale for their suitability as focuses of vaccine efforts.

One of these supersites, the CD4 supersite, is the site of binding for the CD4 receptor on the HIV-1 gp120 envelope glycoprotein. All primate immunodeficiency viruses recognize CD4 as the primary attachment molecule on the cell surface (Hoxie et al., 1988; McClure et al., 1987) and therefore, despite the great genomic and hence antigenic variation between HIV-1 strains, the CD4bs is relatively well conserved (Kwong et al., 1998; Lyumkis et al., 2013; Pancera et al., 2014). Potent broadly neutralizing CD4-binding-site (CD4bs) antibodies are frequently observed during the chronic stage of infection (Binley et al., 2008; Li et al., 2007; Lynch et al., 2012; Pancera et al., 2014; Walker et al., 2010), and numerous CD4bs antibodies have been identified (Burton et al., 1994; Corti et al., 2010; Georgiev et al., 2013; Liao et al., 2013; Scheid et al., 2011; Wu et al., 2010; Wu et al., 2011; Zhu et al., 2013). Analysis of co-crystal structures of core gp120s with three of these CD4bs antibodies, b12, VRC01, and CH103, reveal distinct modes of structural interaction (Liao et al., 2013; Zhou et al., 2010; Zhou et al., 2007), all of which involve substantial interactions with the conformationally invariant gp120-outer domain.

Additional antibody co-crystal structures (Zhou et al., 2013), however, showed CD4bs antibodies from different donors could have similar modes of recognition and similar B cell ontogenies – suggesting that the repertoire of effective CD4bs antibodies might be limited. Because an understanding of the variation in binding characteristics of antibodies specific for a supersite is expected to provide insight regarding how such antibodies might be induced in the general population, we sought to study antibody recognition of the CD4 supersite in multiple donors. We used antigen-specific probes to isolate CD4bs antibodies from diverse germline V_H genes. We determined co-crystal structures with the HIV-1-Env gp120 glycoprotein for these and for previously identified antibodies HJ16, 1B2530, 8ANC131 and 8ANC134 (Corti et al., 2010; Scheid et al., 2011), and characterized B cell ontogenies and paratope chemistries. The repeated observation of similar CD4bs antibodies in 14 donors provided a means to delineate the repertoire for effective recognition of the CD4 supersite. The results define structural geometries, recognized surfaces, paratope chemistries, and developmental pathways of CD4bs recognition, thereby providing a

population-level understanding of antibodies targeting the CD4 supersite as well as a catalogue from which to choose optimal templates for vaccine re-elicitation.

RESULTS

Identification of CD4bs antibodies with diverse germline origin genes

To provide a more comprehensive view for how human antibodies recognize the CD4 supersite, we sought to identify CD4bs antibodies from additional donors. In particular we were interested in determining whether highly effective neutralizing antibodies could originate from heavy chain germline genes other than VH1-2 or VH1-46, the germline origin genes from which virtually all previously identified effective CD4bs antibodies derive. Sera from donors 44, C38, and Z258 showed a substantial reduction in neutralization when adsorbed with the RSC3 probe, a modified core gp120 designed to retain only the outer domain contact of CD4 (Wu et al., 2010). With donor 44, we used RSC3 sorting (Wu et al., 2010) and PCR recovery of individual B cell antibody variable regions (Scheid et al., 2009; Tiller et al., 2008) to isolate an antibody named “44-VRC13.01” (named for “donor-antibody lineage.clone”; after the first mention of the complete antibody name, we refer to each antibody by its lineage name) (Figure S1). VRC13 utilized a V_H gene derived from VH1-69 (Figure S1) and neutralized 82% of circulating HIV-1 isolates (Table S1). From donor C38, we isolated two antibodies: C38-VRC16.01 and C38-VRC18.02 (Figure S1). VRC16 utilized a V_H gene derived from VH3-23 and neutralized 58% of HIV-1 strains; VRC18 utilized a V_H gene derived from VH1-2, was highly similar to an NGS-derived antibody from donor C38 (Zhu et al., 2013), and neutralized 67% of HIV-1 strains (Table S1). From donor Z258, we isolated antibody Z258-VRC27.01. This antibody utilized a V_H gene derived from VH1-2 and neutralized 78% of HIV-1 (Figure S1, Table S1). Altogether, we identified four potent and broadly neutralizing CD4bs antibodies, two of which were derived from V_H genes not previously observed in effective CD4bs antibodies.

Two types of CD4bs antibody recognition

To define the structural modes of antibody recognition, we produced antigen-binding fragments and crystallized these in complex with extended core versions of the HIV-1 gp120 envelope glycoprotein (Kwon et al., 2012). In addition to the four newly identified antibodies, we determined structures for antibodies from three donors with broadly neutralizing antibodies that had not been characterized structurally: the VH3-30-derived antibody HJ16 from donor 242315 (Corti et al., 2010; North et al., 2011) as well as the VH1-46-derived antibodies 1B2530 from donor RU1 and 8ANC131 and 8ANC134 from donor RU8 (Scheid et al., 2011). These 8 new structures (Figure 1, Table S2) from 7 distinct B cell lineages nearly double the number of lineages with structurally defined CD4bs antibody-gp120 complex structures (Table S3).

Structures of HIV-1 gp120 with antibodies from VH1-2 germline (VRC18 and VRC27) or from VH1-46 germline (1B2530, 8ANC131, and 8ANC134) revealed antibody interfaces dominated by the heavy chain second complementarity determining region (CDR H2) (Figure 2A). This “type” or mode of recognition for both VH1-2-and VH1-46-derived antibodies was very similar, although the binding angles of VH1-46-derived antibodies

relative to that of CD4 for 8ANC131 and 8ANC134 were on the outskirts of the strict confines of the VH1-2-derived antibodies (Figure 2B). By contrast, structures of antibodies from germlines other than VH1-2 or VH1-46 (VRC13, VRC16 and HJ16) revealed antibody interfaces dominated by CDR H3, which in each case contributed ~75% of the heavy chain interface (Figure 2A, Table S4). Overall, structural analysis revealed broadly neutralizing CD4bs antibodies to fall into two distinct types: CDR H3-dominated or V_H-gene-restricted, and also provided characteristic features for each type of antibody recognition (Table S3).

Conserved geometry of CD4bs recognition

Despite type-specific features, gp120-binding orientations of the eight newly defined antibodies were similar to each other and to previously determined structures from eight donors (Georgiev et al., 2013; Liao et al., 2013; Wu et al., 2011; Zhou et al., 2010; Zhou et al., 2013) (Figure 2C). For the 15 unique broadly neutralizing CD4bs lineages, the heavy chain comprised the major interactive component (77±10% of the interface). For all 15, the light chain was oriented towards the viral membrane (Figure 2D, Figure S2). Antibodies targeting the CD4bs were constrained geometrically both in latitudinal accessibility, which defines freedom between viral and host cell membranes, and in longitudinal accessibility, which defines freedom within the plane of the membrane (relative to the viral spike, the latitudinal axis is perpendicular to the trimer axis, and the longitudinal axis is parallel to this axis).

While the V_H-gene-restricted antibodies clustered with similar latitudinal angles, the four antibodies of the CDR H3-dominated type each showed latitudes, which were similar to that of CD4 (Figure 2C, left and upper right panels). The constraint in longitude was also pronounced (Figure 2C, middle and lower right panels), with most longitudes within 20°. Overall, the restriction in binding orientation appeared to be substantially greater than observed with antibodies against model antigens such as hen-egg white lysozyme (Braden et al., 1994; Desmyter et al., 1996; Padlan et al., 1989) or against other supersites of HIV-1 vulnerability, such as the membrane-proximal external region on gp41, where antibodies 2F5, 4E10 and 10E8 have divergent binding orientations (Cardoso et al., 2005; Huang et al., 2012; Ofek et al., 2004), or the glycan-V3 supersite on gp120, where longitudinal approach angles ranged from 15 to 95 degrees among four representative antibodies (PGT122, PGT128, PGT135 and 2G12) (Calarese et al., 2003; Julien et al., 2013; Kong et al., 2013; Pejchal et al., 2011)(Figure S3).

To gain an overall understanding of the relationship between breadth of neutralization and binding orientation, we compared the orientation of CD4bs antibodies relative to the most effective CD4bs antibodies thus far developed, modified somatic variants of the VRC01-lineage such as antibody 45–46m2 or antibody VRC07-523 (Diskin et al., 2013; Diskin et al., 2011; Rudicell et al., 2014) (PDB 4JKP and 4OLW). For this analysis, we added three CDR H3-dominated recognizers – b12, b13, and F105 – to the current panel of 16 antibodies (Chen et al., 2009; Zhou et al., 2007). Strong correlation between antibody orientation and neutralization breadth was observed ($p<0.0001$, $R^2=0.64$), with the VH1-2-derived antibodies which were the most similar in angular orientation to antibodies 45–46m2 and VRC07-523 also showing the highest breadth, and these were followed by VH1-46

antibodies and CDR H3-dominated recognizers (Figure 3, upper panel). Separate correlations of CDR H3- dominated and V_H-gene-restricted CD4bs relative to the most effective antibody of each type also showed strong correlation (Figure 3, middle and lower panel). Altogether, effective CD4bs antibodies shared highly similar orientations, both in terms of overall antibody-angle of approach and in terms of heavy-light chain orientation relative to the spike (Figure 2 and 3). However, the two different types of antibodies –CDR H3-dominated and V_H-gene-restricted– correlated better with breadth when treated as separate groups, with CD4bs antibodies clustering around two optimal structural modes of recognition, which were embodied by the most effective antibodies of each type (Figure 2 and 3).

B cell ontogenies

In addition to type, which reflects structural mode of recognition, CD4bs antibodies can be delineated by class, which further categorizes antibodies by their B cell ontogeny (Kwong and Mascola, 2012; West et al., 2014). B cell ontogeny accounts for genetic similarities in developmental pathways and also includes maturation processes such as affinity for antigens that initiate B cell maturation and degree of affinity maturation required for neutralization breadth. Thus a single type of recognition may be achieved by different B cell ontogenies, resulting in different classes of antibodies (Table S3). To define the class of each of the CD4bs antibodies, we studied their ontogenies.

The ontogenies of VH1-2-derived CD4bs antibodies have been defined previously. As a group they are unified by (i) very weak to undetectable binding to gp120 of germline Vgene revertants of heavy and light chain in which the CDR H3 or L3 are mature (gHgL) (Jardine et al., 2013; Klein et al., 2013; McGuire et al., 2013; Mouquet et al., 2010; Scheid et al., 2011; Zhou et al., 2010), (ii) similarities in heavy chain evolution (Wu et al., 2011), and (iii) a specific light chain sequence signature (West et al., 2012; Zhou et al., 2013). These characteristics define the VRC01 class of neutralizing antibodies, named for the first member of this class, VRC01 (Wu et al., 2010), from donor 45 (Wu et al., 2015). Among the new antibodies described here, VRC18 and VRC27 are members of the VRC01 class.

When we analyzed the binding of gHgL revertants of the VH1-46-derived antibodies, 8ANC131 and 1B2530, to a panel of full-length gp120s, no detectable binding was observed, (Figure 4A), similar to the behavior observed for VH1-2-derived VRC01 class members (Scheid et al., 2011; Zhou et al., 2010). Cross-donor phylogenetic analysis (Wu et al., 2011) indicated that the VH1-46 derived antibodies from donor RU1 and RU8 evolved with sufficient similarity to allow the identification of 8ANC131 sequences with 1B2530 sequence similarity and vice-versa (Figure 4B, Table S5). We did not observe a specific heavy or light chain signature. Moreover, when we analyzed immunogens capable of binding the gHgL of VH1-2-derived antibodies (McGuire et al., 2013), we found that the mature forms of antibodies 1B2530 and 8ANC131 bound well to these immunogens, but the gHgL of VH1-46-derived antibodies were unable to bind (Figure S4). Thus, while the VH1-46-derived antibodies were similar to those from the VRC01 class, the preponderance of ontological features indicated that VH1-46-derived antibodies form a separate class,

which we named the 8ANC131 class, after the most effective member of this class (Scheid et al., 2011).

For the CDR H3-dominated antibodies, only the ontogeny of the CH103 antibody has been analyzed in detail previously (Liao et al., 2013). None of the four CDR H3-dominated antibodies analyzed here utilized the same origin genes (V_H, D, J_H, $V_{L/K}$, and $J_{L/K}$), except CH103 and VRC13, which shared the same J_λ gene; however, because the light chain J-region did not contribute substantially to recognition with either CH103 or VRC13, the J_λ-usage was likely not critical to the ontogeny of these antibodies. We tested the recognition of gHgL versions of the four CDR H3-dominated antibodies: the gHgL of VRC13 and of VRC16 showed weak and moderate binding to several gp120s, while gHgL of CH103 and HJ16 showed no detectable binding (Figure 4A). In terms of heavy chain evolution, donor samples for B cell sequencing were available from donors 44 and C38, the sources of antibodies VRC13 and VRC16, respectively. Cross-donor analysis with heavy chain sequences showed no similarities in evolution between VRC13 and VRC16, or between these antibodies and any of the sequences from V_H-gene-restricted donors (Figure 4B). Finally, we could not identify any sequence signatures in the paratopes of the CDR H3-dominated antibodies. In light of these data on gene origin, gHgL recognition, heavy chain evolution, and sequence signature, we conclude that antibodies CH103, HJ16, VRC13, and VRC16 each have different B cell ontogenies and therefore represent separate antibody classes (Figure 4C and Table S3).

Epitope characteristics of CD4bs antibodies

To define the HIV-1-Env surface recognized by highly effective antibodies from 14 donors, we analyzed their epitopes. Recognized surfaces overlapped considerably, although substantial variation was observed with antibodies encoding CDR H3-dominated recognition. For example, HJ16 recognized an epitope that extended towards the viral membrane, and shared less than 50% overlap in recognized Env surface with VRC13. For the V_H-gene-restricted antibodies, epitope surfaces revealed a characteristic discontinuity near the center of the epitope, a feature shared with CD4 (Figure 5A, B). This discontinuity was not observed for antibodies with CDR H3-dominated recognition, where the penetrating CDR H3 loops formed contiguous complementary molecular surfaces. To determine whether these differences in recognition could be detected functionally, we analyzed the neutralization fingerprints (Georgiev et al., 2013) for all 16 CD4bs antibodies on a panel of 178 genetically diverse viruses (Figure 5C). While the neutralization profile of CD4bs antibodies segregated from antibodies targeting other Env sites, within the CD4bs cluster the most divergent were the VH1-46-derived and CDR H3-dominated antibodies, with 1B2530 and HJ16 falling outside of the main CD4bs cluster. The remaining members of the CD4bs classes were interleaved. To provide a per-residue understanding of the CD4 supersite, we combined recognized epitope with neutralization potency to construct a residue-level picture of the CD4 supersite (Figure 5D, Figure S5). Overall, despite differences in structural mode of recognition and class, all of the CD4bs antibodies displayed general similarities in terms of recognized epitope and profile of viruses neutralized.

Paratope characteristics of CD4bs antibodies

To understand how these antibodies recognize the CD4 supersite, we analyzed their paratopes. First, we structurally aligned gp120 components from co-crystal structures and analyzed known hot spots of CD4 interaction (Ryu et al., 1990; Wang et al., 1990) (Figure 6) (for clarity, from this point forwards, residues are displayed with a subscript defining the molecule). Within domain 1 of CD4, $Phe43_{CD4}$ makes contacts with the "Phe43 pocket" on gp120 and forms hydrophobic interactions with $Glu370_{gp120}$, $Ile371_{gp120}$, and $Trp427_{gp120}$ and backbone contacts with residues 425_{gp120} and 473_{gp120} (Figure 6A, Table S6). Interestingly, a similar hydrophobic interaction was observed in some of the VH1-2-derived VRC01-class antibodies, including $Trp54_{VRC\text{-}PG20}$, $Phe54_{12A21}$ and $Phe54_{VRC27}$. Despite this interaction being highly favorable (Diskin et al., 2011; Rudicell et al., 2014), it was not preserved in other members of the VRC01 class. For example, with VRC01, residue 54_{VRC01} is a glycine, and no hydrophobic residue substitutes for this interaction (Figure 6A). For the VH1-46-derived antibodies, no similar residue is found in 8ANC131, but for antibody 1B2530, $Arg54_{1B2530}$ engages the gp120 Phe43 pocket in a manner similar to VH1-2 antibody VRC23. Meanwhile, with the CDR H3-dominated antibodies, in VRC16 the phenyl ring of $Tyr100E_{VRC16}$ is oriented almost identically to that of $Phe43_{CD4}$, whereas in CH103, HJ16, and VRC13, no similar interactions are observed; indeed HJ16 does not even interact with the Phe43 pocket (Figure S6). Thus the specific chemical interactions at the Phe43 pocket of gp120 appeared to be highly variable.

In terms of the other highly favorable interaction within domain 1 of CD4, $Arg59_{CD4}$ forms electrostatic interactions with $Asp368_{gp120}$ (Figure 6B). With all of the V_H-gene-restricted type antibodies, both from VH1-2 and VH1-46 origins, $Arg71_{heavy\ chain}$ makes similar interactions. Notably, the combination of a CDR H2-dominated interface along with use of $Arg71_{heavy\ chain}$ may explain the restricted V_H-gene usage of this antibody type. Many common V_H genes encode $Arg71_{heavy\ chain}$, but this residue is often buried between CDR H2 and CDR H1 (North et al., 2011). VH1-2 and VH1-46 seem to possess CDR H2 sequence features (such as $Pro52A_{heavy\ chain}$) that lead to a CDR H2 conformation that is compatible with gp120-binding and which exposes $Arg71_{heavy\ chain}$ (see Germline gene usage of the VH-gene restricted antibodies in Supplemental Information). In the CDR H3-dominated antibodies, both CH103 and VRC13 use Arg residues ($Arg97_{CH103}$ and $Arg96_{VRC13}$) to mimic the interactions of $Arg59_{CD4}$, but antibody HJ16 has no equivalent interactions, and antibody VRC16 uses a His side chain to approximate this interaction (Figure 6B). Thus the specific chemical interactions with $Asp368_{gp120}$ appeared to be mostly, though not entirely, conserved.

To provide an overall understanding of the recognition surface, we analyzed paratope chemistry utilized in recognizing the CD4 supersite (Figure 7, Table S7). We observed substantial inter-class differences, with CDR H3-dominated antibodies displaying especially varied binding surfaces and interactive chemistry. We also examined intra-class differences between different donors with antibodies derived from common V_H genes (Figure 7B). Among members of the VRC01 class (Figure 7B, left panels), paratope chemistry and atom type (Petrey and Honig, 2000) were similar, despite the paratope being altered by substantial somatic hypermutation. Notably this hypermutation occurred in similar regions of the

paratope, likely reflecting similarities in ontogeny and in requirements to achieve optimal recognition. Substantial diversity, however, was observed among antibodies of the 8ANC131 class from different donors (Figure 7B, right panels).

Thus highly effective CD4bs antibodies, even those of the same B cell ontogeny, can develop distinct paratope chemistry. These differences in paratope chemistry indicate that the immune system can find diverse solutions to the recognition of the same target epitope.

DISCUSSION

While antibodies of the human immune system can recognize epitopes in diverse ways, repeated observations in 14 donors of similar geometries of recognition and similar B cell ontogenies suggest the repertoire for broad neutralization to be relatively limited. One potential explanation for this limitation is that HIV-1 Env is so well protected from antibody recognition that the humoral immune system can develop effective recognition – even against the more prevalently recognized supersites of Env vulnerability – through only a few pathways.

It may be important to identify critical factors that constrain the development of effective recognition, and one way to do this is to analyze the recognition of multiple antibodies that target the same supersite at the population level. Elements of diversity between these antibodies would indicate factors that allow the immune system to develop multiple solutions; elements of similarity would indicate dominant constraining factors. In the case of the CD4 supersite, we observed the overall geometry of antibody recognition to be highly similar (Figure 7A); this suggested a dominant constraining factor for the elicitation of CD4bs antibodies to be paratope accessibility at the recessed CD4 supersite on functional viral spikes (Lyumkis et al., 2013; Pancera et al., 2014).

The 14 donors analyzed here define our current understanding of the human antibody repertoire that can effectively recognize the CD4 supersite on HIV-1. While surrounded by glycan, the surface that binds CD4 is itself free of glycan (Kwong et al., 1998): indeed it is the only epitope cluster on the HIV-1-Env spike that is both glycan-free and not membraneproximal (Pancera et al., 2014). The V_H-gene-restricted classes that successfully target this site each appear in multiple donors and share evolutionary similarities, suggesting developmental pathways accessible to the general population. By contrast, the CDR H3-dominated classes each appear in a single donor and show no detectable evolutionary similarity or sequence signature, suggesting origins that are stochastic and therefore not shared between different individuals. Because the germline-reverted (gHgL) versions of the V_H-gene-restricted and CDR H3-dominated antibodies showed different binding behaviors to gp120, we assessed their B cell activation properties to provide insight into early development. Calcium flux experiments indicated that B cell triggering could occur with gHgL versions of VRC13, but not VRC01 (Figure S4), demonstrating differences in ontogeny whereby germline versions of some CDR H3-dominated antibodies could trigger B cell activation more efficiently than germline-reverted versions of antibodies from V_H-gene-restricted classes. This was supported by the binding of the germline-reverted version of the CDR H3-dominated VRC13 and VRC16 (Figure 2), by the autologous-virus specific

binding of the unmutated common ancestor of the CDR H3-dominated CH103 (Liao et al., 2013), and by the lack of binding for germline-reverted versions of V_H-gene-restricted antibodies (Figure 4, Figure S4) (Jardine et al., 2013; McGuire et al., 2013; Zhou et al., 2010). Finally the inability of germline-reverted VH1-46 antibodies to bind immunogens, which had been developed to recognize germline-reverted VH1-2 antibodies, indicated that different classes of V_H-gene-restricted antibodies may require different immunogens. Together, the results suggest that distinct immunogens may be required to stimulate the development of the different types and classes of broadly neutralizing antibodies that recognize the CD4 supersite.

Overall, the CD4bs antibody analysis described here, the first comprehensive analysis of antibody recognition for a supersite of HIV-1 vulnerability, provides a framework linking structural mode of antibody recognition (type) with B cell ontogeny (class) and paratope chemistry in 14 donors (Table S3). Serum from these donors displayed a range of potencies, though with breadths generally in the upper range (Figure S7). This population-level analysis provides insight into constraining factors (e.g. from similarities in elicited antibodies) as well as the ease by which the immune system can replicate a particular lineage pathway (e.g. from similarities in ontogeny). The results indicate that the repertoire for effective recognition of the CD4 supersite consists of antibodies with diverse paratopes that cluster around two solutions: one achieved by V_H-gene-restricted ontogenies and the other achieved by CDR H3- dominated ontogenies. The V_H-gene-restricted solution, embodied by antibodies 45–46m2 and VRC07-523 (Diskin et al., 2013; Rudicell et al., 2014), uses the CDR H2 region to mimic the C'' recognition of CD4 (Kwong et al., 1998), though with a different latitudinal orientation to accommodate the light chain (Zhou et al., 2010). The CDR H3-dominated solution, embodied by antibody VRC13 isolated here, uses the CDR H3 region to recognize the CD4 supersite, with the same latitudinal angle as CD4. It will be interesting to see if additional broadly neutralizing CD4bs antibodies will continue to cluster around these two solutions and whether other highly effective solutions to the problem of antibody recognition of the CD4 supersite can be found.

EXPERIMENTAL PROCEDURES

Human Specimens

Donors 44, C38 and Z258 participated in NIAID protocols (Doria-Rose et al., 2009) at the National Institutes of Health, Bethesda, MD, USA. HIV infection was documented by HIV-1/2 immunoassay. The donors were chronically infected and had not initiated antiretroviral treatment at the time of sample collection. All human samples were collected with informed consent under clinical protocols approved by the appropriate institutional review board (IRB).

Isolation and Expression of Antibody 44-VRC13.01, C38-VRC16.01, C38-VRC18.02 and Z258-VRC27.01

Antigen-specific memory B cells from donors 44, C38 and Z258 were isolated with Avitagged RSC3 and ΔRSC3 and single-cell sorted on a FACS Aria II as described previously (Wu et al., 2010). (Extended Experimental Procedures)

Production and Purification of HIV-1 Env Protein and Antibodies

HIV-1 gp120 proteins were produced in GNTI −/− cells and purified as described previously (Zhou et al., 2010). Human antibodies were expressed in HEK293F cells and purified by Protein A affinity columns. Antigen-binding fragments (Fab) of antibodies were prepared by overnight Lys-C digestion at 37°C with a IgG:Lys-C ratio of 4000:1 (w/w), and sequential purification over Protein A and size exclusion columns.

Neutralization Assays

Single round of replication Env-pseudoviruses were prepared, titered and used to infect TZM-bl target cells as described previously (Montefiori, 2009) (Extended Experimental Procedures and Table S1).

Formation of Protein Complexes, Crystallization, and Data Collection

The gp120-antibody complexes were formed by mixing deglycosylated HIV-1 gp120 with antibody Fab in a 1:1.2 molar ratio. The complexes were purified by size exclusion chromatography. Fractions with gp120-antibody complexes were concentrated to ~10 mg/ml for crystallization experiments. Crystallization conditions for all gp120-Fab complexes were obtained robotically and manually optimized in hanging drops (Extended Experimental Procedures).

Structure Determination and Refinement

All structure was solved by molecular replacement with Phaser (McCoy et al., 2007). Iterative model building and refinement procedures were carried out using Coot (Emsley and Cowtan, 2004) and Phenix (Adams et al., 2010) (Extended Experimental Procedures and Table S2).

Bioinformatics Analysis of Antibody Neutralization and 454 Sequencing Data

The neutralization fingerprint of antibodies were analyzed with procedures described previously (Georgiev et al., 2013). High throughput B cell sequencing of donor samples, bioinformatics processing of sequencing data and cross-donor phylogenetic analysis of antibody sequences were carried out with similar procedures as described (Wu et al., 2011; Zhu et al., 2012) (Extended Experimental Procedures and Table S5)

Structural Analysis

All antibody complexes were aligned over the outer domain of HIV-1 gp120 to gain a common reference frame for further comparison of the modes of recognition to the CD4-binding site. The BG505.664 SOSIP crystal structure (PDB ID: 4TVP) was used to analyze antibody recognition on the HIV-1 viral spike (Pancera et al., 2014). (Extended Experimental Procedures).

Supplementary Material

Refer to Web version on PubMed Central for supplementary material.

Authors

Tongqing Zhou[1,*], Rebecca M. Lynch[1,*], Lei Chen[1,*], Priyamvada Acharya[1,*], Xueling Wu[1], Nicole A. Doria-Rose[1], M. Gordon Joyce[1], Daniel Lingwood[1], Cinque Soto[1], Robert T. Bailer[1], Michael J. Ernandes[1], Rui Kong[1], Nancy S. Longo[1], Mark K. Louder[1], Krisha McKee[1], Sijy O'Dell[1], Stephen D. Schmidt[1], Lillian Tran[1], Zhongjia Yang[1], Aliaksandr Druz[1], Timothy S. Luongo[1], Stephanie Moquin[1], Sanjay Srivatsan[1], Yongping Yang[1], Baoshan Zhang[1], Anqi Zheng[1], Marie Pancera[1], Tatsiana Kirys[1], Ivelin S. Georgiev[1], Tatyana Gindin[2], Hung-Pin Peng[3], An-Suei Yang[3], NISC Comparative Sequencing Program[4], James C. Mullikin[4], Matthew D. Gray[5], Leonidas Stamatatos[5], Dennis R. Burton[6,7], Wayne C. Koff[8], Myron S. Cohen[9], Barton F. Haynes[10], Joseph P. Casazza[1], Mark Connors[11], Davide Corti[12,13], Antonio Lanzavecchia[13], Quentin J. Sattentau[14], Robin A. Weiss[15], Anthony P. West Jr.[16], Pamela J. Bjorkman[16,17], Johannes F. Scheid[18], Michel C. Nussenzweig[18,19], Lawrence Shapiro[1,2], John R. Mascola[1,#], and Peter D. Kwong[1,#]

Affiliations

[1]Vaccine Research Center, National Institute of Allergy and Infectious Diseases, and National Institutes of Health, Bethesda, Maryland 20892, USA [2]Department of Biochemistry & Molecular Biophysics and Department of Systems Biology, Columbia University, New York, NY 10032, USA [3]Genomics Research Center, Academia Sinica, and Institute of Biomedical Informatics, National Yang-Ming University, Taipei, Taiwan 11221 [4]NIH Intramural Sequencing Center, National Human Genome Research Institute, National Institutes of Health, Bethesda, Maryland 20892, USA [5]Vaccine and Infectious Disease Division, Fred Hutchinson Cancer Research Center, Seattle, WA 98109, USA [6]Department of Immunology and Microbial Science, International AIDS Vaccine Initiative Neutralizing Antibody Center, Center for HIV/AIDS Vaccine Immunology and Immunogen Discovery, The Scripps Research Institute, La Jolla, CA 92037, USA [7]Ragon Institute of Massachusetts General Hospital, Massachusetts Institute of Technology and Harvard University, Boston, MA 02142, USA [8]International AIDS Vaccine Initiative, New York, NY 10038, USA [9]Departments of Medicine, Epidemiology, Microbiology and Immunology, University of North Carolina at Chapel Hill, Chapel Hill, North Carolina 27599, USA [10]Duke University Human Vaccine Institute, Departments of Medicine, Surgery, Pediatrics and Immunology, Duke University School of Medicine, and the Center for HIV/AIDS Vaccine Immunology-Immunogen Discovery at Duke University, Durham, North Carolina 27710, USA [11]HIV-Specific Immunity Section, Laboratory of Immunoregulation, National Institute of Allergy and Infectious Diseases, and National Institutes of Health, Bethesda, Maryland 20892, USA [12]Humabs BioMed SA, Via Mirasole 1, 6500 Bellinzona, Switzerland [13]Institute for Research in Biomedicine, Università della Svizzera Italiana, Via Vincenzo Vela 6, 6500 Bellinzona, Switzerland [14]Sir William Dunn School of Pathology, University of Oxford, Oxford, United Kingdom [15]Division of Infection & Immunity, University College London, Gower Street, London WC1E 6BT, UK [16]Division of Biology and

Biological Engineering, California Institute of Technology, Pasadena, CA 91125, USA [17]Howard Hughes Medical Institute, California Institute of Technology, Pasadena, CA 91125, USA [18]Laboratory of Molecular Immunology, The Rockefeller University, New York, NY 10065, USA [19]Howard Hughes Medical Institute, The Rockefeller University, New York, NY 10065, USA

ACKNOWLEDGMENTS

We thank members of the Structural Biology Section and Structural Bioinformatics Core, Vaccine Research Center, for discussions and comments on the manuscript, and B. Honig for structural biology mentorship. We thank J. Baalwa, D. Ellenberger, F. Gao, B. Hahn, K. Hong, J. Kim, F. McCutchan, D. Montefiori, L. Morris, J. Overbaugh, E. Sanders-Buell, G. Shaw, R. Swanstrom, M. Thomson, S. Tovanabutra, C. Williamson, and L. Zhang for contributing the HIV-1 Envelope plasmids used in our neutralization panel. The authors acknowledge the contributions of the Center for HIV/AIDS Vaccine Discovery (CHAVI) Clinical Core Team. Support for this work was provided by the Intramural Research Program of the Vaccine Research Center, National Institute of Allergy and Infectious Diseases (NIAID), National Institutes of Health, by the Howard Hughes Medical Institute (MCN and PJB are investigators), and by grants from the Division of AIDS, NIAID, National Institutes of Health (AI037526, AI072529, AI0678501, P01 AI094419, P01 AI100148, P01 AI104722, and 1UM1 AI100663 and UM1 AI100645), from The Bill and Melinda Gates Foundation (Collaboration for AIDS Vaccine Discovery Grant IDs 38637 and 1040753), and from the International AIDS Vaccine Initiative's (IAVI's) Neutralizing Antibody Consortium. IAVI's work is made possible by support from many donors including: the Bill & Melinda Gates Foundation; the Ministry of Foreign Affairs of Denmark; Irish Aid; the Ministry of Finance of Japan; the Ministry of Foreign Affairs of the Netherlands; the Norwegian Agency for Development Cooperation (NORAD); the UK Department for International Development (DFID): and the United States Agency for International Development (USAID). The full list of IAVI donors is available at http://www.iavi.org. Use of sector 22 (Southeast Region Collaborative Access team) at the Advanced Photon Source was supported by the US Department of Energy, Basic Energy Sciences, Office of Science, under contract number W-31-109-Eng-38.

References

Adams PD, Afonine PV, Bunkoczi G, Chen VB, Davis IW, Echols N, Headd JJ, Hung LW, Kapral GJ, Grosse-Kunstleve RW, et al. PHENIX: a comprehensive Python-based system for macromolecular structure solution. Acta Crystallogr D Biol Crystallogr. 2010; 66:213–221. [PubMed: 20124702]

Binley JM, Lybarger EA, Crooks ET, Seaman MS, Gray E, Davis KL, Decker JM, Wycuff D, Harris L, Hawkins N, et al. Profiling the specificity of neutralizing antibodies in a large panel of plasmas from patients chronically infected with human immunodeficiency virus type 1 subtypes B and C. Journal of virology. 2008; 82:11651–11668. [PubMed: 18815292]

Braden BC, Souchon H, Eisele JL, Bentley GA, Bhat TN, Navaza J, Poljak RJ. Three-dimensional structures of the free and the antigen-complexed Fab from monoclonal anti-lysozyme antibody D44.1. Journal of molecular biology. 1994; 243:767–781. [PubMed: 7966295]

Burton DR, Pyati J, Koduri R, Sharp SJ, Thornton GB, Parren PW, Sawyer LS, Hendry RM, Dunlop N, Nara PL, et al. Efficient neutralization of primary isolates of HIV-1 by a recombinant human monoclonal antibody. Science. 1994; 266:1024–1027. [PubMed: 7973652]

Calarese DA, Scanlan CN, Zwick MB, Deechongkit S, Mimura Y, Kunert R, Zhu P, Wormald MR, Stanfield RL, Roux KH, et al. Antibody domain exchange is an immunological solution to carbohydrate cluster recognition. Science. 2003; 300:2065–2071. [PubMed: 12829775]

Cardoso RM, Zwick MB, Stanfield RL, Kunert R, Binley JM, Katinger H, Burton DR, Wilson IA. Broadly neutralizing anti-HIV antibody 4E10 recognizes a helical conformation of a highly conserved fusion-associated motif in gp41. Immunity. 2005; 22:163–173. [PubMed: 15723805]

Chen L, Kwon YD, Zhou T, Wu X, O'Dell S, Cavacini L, Hessell AJ, Pancera M, Tang M, Xu L, et al. Structural basis of immune evasion at the site of CD4 attachment on HIV-1 gp120. Science. 2009; 326:1123–1127. [PubMed: 19965434]

Corti D, Langedijk JP, Hinz A, Seaman MS, Vanzetta F, Fernandez-Rodriguez BM, Silacci C, Pinna D, Jarrossay D, Balla-Jhagjhoorsingh S, et al. Analysis of memory B cell responses and isolation of

novel monoclonal antibodies with neutralizing breadth from HIV-1-infected individuals. PloS one. 2010; 5:e8805. [PubMed: 20098712]

Desmyter A, Transue TR, Ghahroudi MA, Thi MH, Poortmans F, Hamers R, Muyldermans S, Wyns L. Crystal structure of a camel single-domain VH antibody fragment in complex with lysozyme. Nature structural biology. 1996; 3:803–811.

Diskin R, Klein F, Horwitz JA, Halper-Stromberg A, Sather DN, Marcovecchio PM, Lee T, West AP Jr, Gao H, Seaman MS, et al. Restricting HIV-1 pathways for escape using rationally designed anti-HIV-1 antibodies. The Journal of experimental medicine. 2013; 210:1235–1249. [PubMed: 23712429]

Diskin R, Scheid JF, Marcovecchio PM, West AP Jr, Klein F, Gao H, Gnanapragasam PN, Abadir A, Seaman MS, Nussenzweig MC, et al. Increasing the potency and breadth of an HIV antibody by using structure-based rational design. Science. 2011; 334:1289–1293. [PubMed: 22033520]

Emsley P, Cowtan K. Coot: model-building tools for molecular graphics. Acta Crystallogr D Biol Crystallogr. 2004; 60:2126–2132. [PubMed: 15572765]

Georgiev IS, Doria-Rose NA, Zhou T, Kwon YD, Staupe RP, Moquin S, Chuang GY, Louder MK, Schmidt SD, Altae-Tran HR, et al. Delineating antibody recognition in polyclonal sera from patterns of HIV-1 isolate neutralization. Science. 2013; 340:751–756. [PubMed: 23661761]

Hoxie JA, Haggarty BS, Bonser SE, Rackowski JL, Shan H, Kanki PJ. Biological characterization of a simian immunodeficiency virus-like retrovirus (HTLV-IV): evidence for CD4-associated molecules required for infection. Journal of virology. 1988; 62:2557–2568. [PubMed: 2839686]

Hraber P, Seaman MS, Bailer RT, Mascola JR, Montefiori DC, Korber BT. Prevalence of broadly neutralizing antibody responses during chronic HIV-1 infection. Aids. 2014; 28:163–169. [PubMed: 24361678]

Huang J, Ofek G, Laub L, Louder MK, Doria-Rose NA, Longo NS, Imamichi H, Bailer RT, Chakrabarti B, Sharma SK, et al. Broad and potent neutralization of HIV-1 by a gp41-specific human antibody. Nature. 2012; 491:406–412. [PubMed: 23151583]

Jardine J, Julien JP, Menis S, Ota T, Kalyuzhniy O, McGuire A, Sok D, Huang PS, MacPherson S, Jones M, et al. Rational HIV immunogen design to target specific germline B cell receptors. Science. 2013; 340:711–716. [PubMed: 23539181]

Julien JP, Cupo A, Sok D, Stanfield RL, Lyumkis D, Deller MC, Klasse PJ, Burton DR, Sanders RW, Moore JP, et al. Crystal structure of a soluble cleaved HIV-1 envelope trimer. Science. 2013; 342:1477–1483. [PubMed: 24179159]

Klein F, Diskin R, Scheid JF, Gaebler C, Mouquet H, Georgiev I, Pancera M, Zhou T, Incesu RB, Fu BZ, et al. Somatic mutations of the immunoglobulin framework are generaly required for broad and potent HIV-1 neutralizing activity. Cell. 2013 *in press*.

Kong L, Lee JH, Doores KJ, Murin CD, Julien JP, McBride R, Liu Y, Marozsan A, Cupo A, Klasse PJ, et al. Supersite of immune vulnerability on the glycosylated face of HIV-1 envelope glycoprotein gp120. Nature structural & molecular biology. 2013; 20:796–803.

Kwon YD, Finzi A, Wu X, Dogo-Isonagie C, Lee LK, Moore LR, Schmidt SD, Stuckey J, Yang Y, Zhou T, et al. Unliganded HIV-1 gp120 core structures assume the CD4-bound conformation with regulation by quaternary interactions and variable loops. Proceedings of the National Academy of Sciences of the United States of America. 2012; 109:5663–5668. [PubMed: 22451932]

Kwong PD, Mascola JR. Human antibodies that neutralize HIV-1: identification, structures, and B cell ontogenies. Immunity. 2012; 37:412–425. [PubMed: 22999947]

Kwong PD, Wyatt R, Robinson J, Sweet RW, Sodroski J, Hendrickson WA. Structure of an HIV gp120 envelope glycoprotein in complex with the CD4 receptor and a neutralizing human antibody. Nature. 1998; 393:648–659. [PubMed: 9641677]

Li Y, Migueles SA, Welcher B, Svehla K, Phogat A, Louder MK, Wu X, Shaw GM, Connors M, Wyatt RT, et al. Broad HIV-1 neutralization mediated by CD4-binding site antibodies. Nat Med. 2007; 13:1032–1034. [PubMed: 17721546]

Liao HX, Lynch R, Zhou T, Gao F, Alam SM, Boyd SD, Fire A, Roskin K, Schramm C, Zhang Z, et al. Co-evolution of a broadly neutralizing HIV-1 antibody and founder virus. Nature. 2013 In press.

Lynch RM, Tran L, Louder MK, Schmidt SD, Cohen M, Members CCT, Dersimonian R, Euler Z, Gray ES, Abdool Karim S, et al. The development of CD4 binding site antibodies during HIV-1 infection. Journal of virology. 2012; 86:7588–7595. [PubMed: 22573869]

Lyumkis D, Julien JP, de Val N, Cupo A, Potter CS, Klasse PJ, Burton DR, Sanders RW, Moore JP, Carragher B, et al. Cryo-EM structure of a fully glycosylated soluble cleaved HIV-1 envelope trimer. Science. 2013; 342:1484–1490. [PubMed: 24179160]

McClure MO, Sattentau QJ, Beverley PC, Hearn JP, Fitzgerald AK, Zuckerman AJ, Weiss RA. HIV infection of primate lymphocytes and conservation of the CD4 receptor. Nature. 1987; 330:487–489. [PubMed: 2446142]

McCoy AJ, Grosse-Kunstleve RW, Adams PD, Winn MD, Storoni LC, Read RJ. Phaser crystallographic software. J Appl Crystallogr. 2007; 40:658–674. [PubMed: 19461840]

McGuire AT, Hoot S, Dreyer AM, Lippy A, Stuart A, Cohen KW, Jardine J, Menis S, Scheid JF, West AP, et al. Engineering HIV envelope protein to activate germline B cell receptors of broadly neutralizing anti-CD4 binding site antibodies. The Journal of experimental medicine. 2013

Montefiori DC. Measuring HIV neutralization in a luciferase reporter gene assay. Methods in molecular biology. 2009; 485:395–405. [PubMed: 19020839]

Mouquet H, Scheid JF, Zoller MJ, Krogsgaard M, Ott RG, Shukair S, Artyomov MN, Pietzsch J, Connors M, Pereyra F, et al. Polyreactivity increases the apparent affinity of anti-HIV antibodies by heteroligation. Nature. 2010; 467:591–595. [PubMed: 20882016]

North B, Lehmann A, Dunbrack RL Jr. A new clustering of antibody CDR loop conformations. Journal of molecular biology. 2011; 406:228–256. [PubMed: 21035459]

Ofek G, Tang M, Sambor A, Katinger H, Mascola JR, Wyatt R, Kwong PD. Structure and mechanistic analysis of the anti-human immunodeficiency virus type 1 antibody 2F5 in complex with its gp41 epitope. Journal of virology. 2004; 78:10724–10737. [PubMed: 15367639]

Padlan EA, Silverton EW, Sheriff S, Cohen GH, Smith-Gill SJ, Davies DR. Structure of an antibody-antigen complex: crystal structure of the HyHEL-10 Fablysozyme complex. Proceedings of the National Academy of Sciences of the United States of America. 1989; 86:5938–5942. [PubMed: 2762305]

Pancera M, Zhou T, Druz A, Georgiev IS, Soto C, Gorman J, Huang J, Acharya P, Chuang GY, Ofek G, et al. Structure and immune recognition of trimeric prefusion HIV-1 Env. Nature. 2014; 514:455–461. [PubMed: 25296255]

Pejchal R, Doores KJ, Walker LM, Khayat R, Huang PS, Wang SK, Stanfield RL, Julien JP, Ramos A, Crispin M, et al. A potent and broad neutralizing antibody recognizes and penetrates the HIV glycan shield. Science. 2011; 334:1097–1103. [PubMed: 21998254]

Petrey D, Honig B. Free energy determinants of tertiary structure and the evaluation of protein models. Protein science : a publication of the Protein Society. 2000; 9:2181–2191. [PubMed: 11152128]

Rudicell RS, Kwon YD, Ko SY, Pegu A, Louder MK, Georgiev IS, Wu X, Zhu J, Boyington JC, Chen X, et al. Enhanced potency of a broadly neutralizing HIV-1 antibody in vitro improves protection against lentiviral infection in vivo. Journal of virology. 2014; 88:12669–12682. [PubMed: 25142607]

Ryu SE, Kwong PD, Truneh A, Porter TG, Arthos J, Rosenberg M, Dai XP, Xuong NH, Axel R, Sweet RW, et al. Crystal structure of an HIV-binding recombinant fragment of human CD4. Nature. 1990; 348:419–426. [PubMed: 2247146]

Scheid JF, Mouquet H, Feldhahn N, Walker BD, Pereyra F, Cutrell E, Seaman MS, Mascola JR, Wyatt RT, Wardemann H, et al. A method for identification of HIV gp140 binding memory B cells in human blood. J Immunol Methods. 2009; 343:65–67. [PubMed: 19100741]

Scheid JF, Mouquet H, Ueberheide B, Diskin R, Klein F, Oliveira TY, Pietzsch J, Fenyo D, Abadir A, Velinzon K, et al. Sequence and structural convergence of broad and potent HIV antibodies that mimic CD4 binding. Science. 2011; 333:1633–1637. [PubMed: 21764753]

Tiller T, Meffre E, Yurasov S, Tsuiji M, Nussenzweig MC, Wardemann H. Efficient generation of monoclonal antibodies from single human B cells by single cell RT-PCR and expression vector cloning. J Immunol Methods. 2008; 329:112–124. [PubMed: 17996249]

Walker LM, Simek MD, Priddy F, Gach JS, Wagner D, Zwick MB, Phogat SK, Poignard P, Burton DR. A limited number of antibody specificities mediate broad and potent serum neutralization in selected HIV-1 infected individuals. PLoS pathogens. 2010; 6:e1001028. [PubMed: 20700449]

Wang JH, Yan YW, Garrett TP, Liu JH, Rodgers DW, Garlick RL, Tarr GE, Husain Y, Reinherz EL, Harrison SC. Atomic structure of a fragment of human CD4 containing two immunoglobulin-like domains. Nature. 1990; 348:411–418. [PubMed: 1701030]

West AP Jr, Diskin R, Nussenzweig MC, Bjorkman PJ. Structural basis for germ-line gene usage of a potent class of antibodies targeting the CD4-binding site of HIV-1 gp120. Proceedings of the National Academy of Sciences of the United States of America. 2012; 109:E2083–E2090. [PubMed: 22745174]

West AP Jr, Scharf L, Scheid JF, Klein F, Bjorkman PJ, Nussenzweig MC. Structural insights on the role of antibodies in HIV-1 vaccine and therapy. Cell. 2014; 156:633–648. [PubMed: 24529371]

Wu X, Yang ZY, Li Y, Hogerkorp CM, Schief WR, Seaman MS, Zhou T, Schmidt SD, Wu L, Xu L, et al. Rational design of envelope identifies broadly neutralizing human monoclonal antibodies to HIV-1. Science. 2010; 329:856–861. [PubMed: 20616233]

Wu X, Zhang Z, Schramm CA, M Joyce G, Kwon YD, Zhou T, Sheng Z, Zhang B, O'Dell S, McKee K, et al. Maturation and diversity of the VRC01-antibody lineage over 15 years of chronic HIV-1 infection. Cell. 2015 *In press*.

Wu X, Zhou T, Zhu J, Zhang B, Georgiev I, Wang C, Chen X, Longo NS, Louder M, McKee K, et al. Focused evolution of HIV-1 neutralizing antibodies revealed by structures and deep sequencing. Science. 2011; 333:1593–1602. [PubMed: 21835983]

Zhou T, Georgiev I, Wu X, Yang ZY, Dai K, Finzi A, Do Kwon Y, Scheid J, Shi W, Xu L, et al. Structural basis for broad and potent neutralization of HIV-1 by antibody VRC01. Science. 2010; 329:811–817. [PubMed: 20616231]

Zhou T, Xu L, Dey B, Hessell AJ, Van Ryk D, Xiang SH, Yang X, Zhang MY, Zwick MB, Arthos J, et al. Structural definition of a conserved neutralization epitope on HIV-1 gp120. Nature. 2007; 445:732–737. [PubMed: 17301785]

Zhou T, Zhu J, Wu X, Moquin S, Zhang B, Acharya P, Georgiev IS, Altae-Tran HR, Chuang GY, Joyce MG, et al. Multidonor analysis reveals structural elements, genetic determinants, and maturation pathway for HIV-1 neutralization by VRC01-class antibodies. Immunity. 2013; 39:245–258. [PubMed: 23911655]

Zhu J, O'Dell S, Ofek G, Pancera M, Wu X, Zhang B, Zhang Z, Program N.C.S. Mullikin JC, Simek M, et al. Somatic Populations of PGT135-137 HIV-1-Neutralizing Antibodies Identified by 454 Pyrosequencing and Bioinformatics. Front Microbiol. 2012; 3:315. [PubMed: 23024643]

Zhu J, Wu X, Zhang B, McKee K, O'Dell S, Soto C, Zhou T, Casazza JP, Mullikin JC, Kwong PD, et al. De novo identification of VRC01 class HIV-1-neutralizing antibodies by next-generation sequencing of B-cell transcripts. Proceedings of the National Academy of Sciences of the United States of America. 2013; 110:E4088–E4097. [PubMed: 24106303]

Highlights

- Population-level analysis revealed only two types of effective CD4bs antibodies.
- Each type, CDR H3-dominated or VH-gene-restricted, had distinct ontogenies.
- Both types could neutralize effectively, each with an optimal angle of approach.
- Despite geometric similarities, paratope chemistries were extremely diverse.

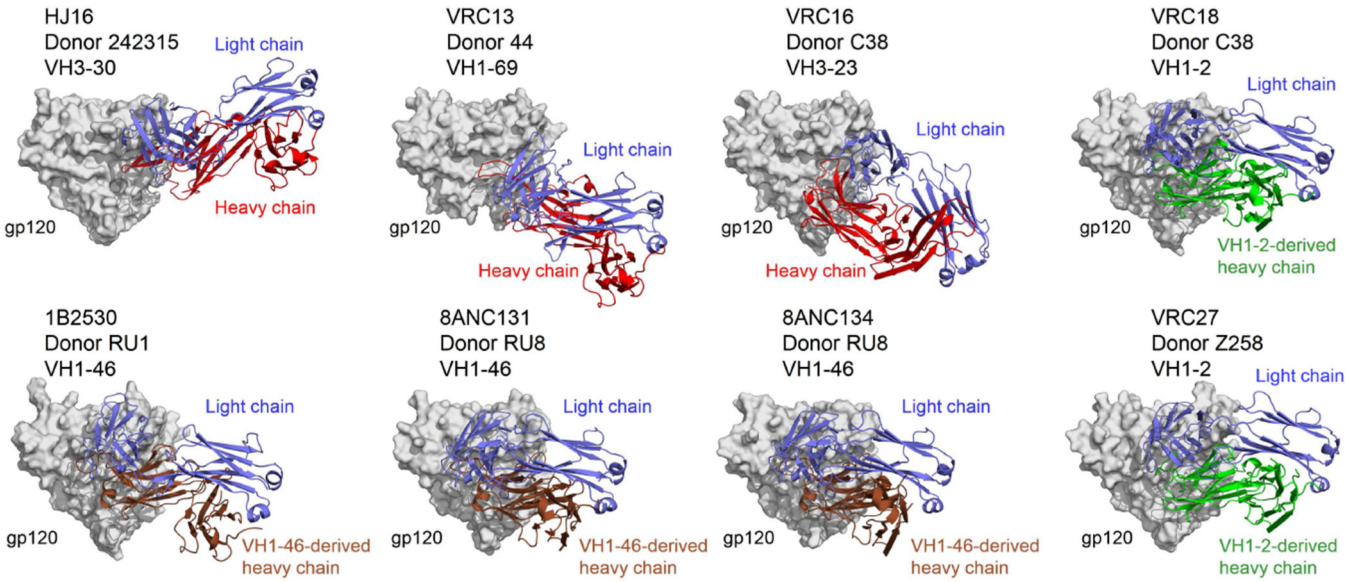

Figure 1. Crystal Structures of Eight CD4bs Antibodies in Complex with HIV-1 gp120 Show Similar Heavy and Light Chain Orientations

Complex structures are shown from a common alignment with gp120 (gray surface representation), with the light chain shown in blue and the heavy chains shown in red, green, and brown for CDR H3-dominated recognizers, VH1-2-derived heavy chains, and VH1-46-derived heavy chains, respectively. See also Figure S1, Table S1 and S2.

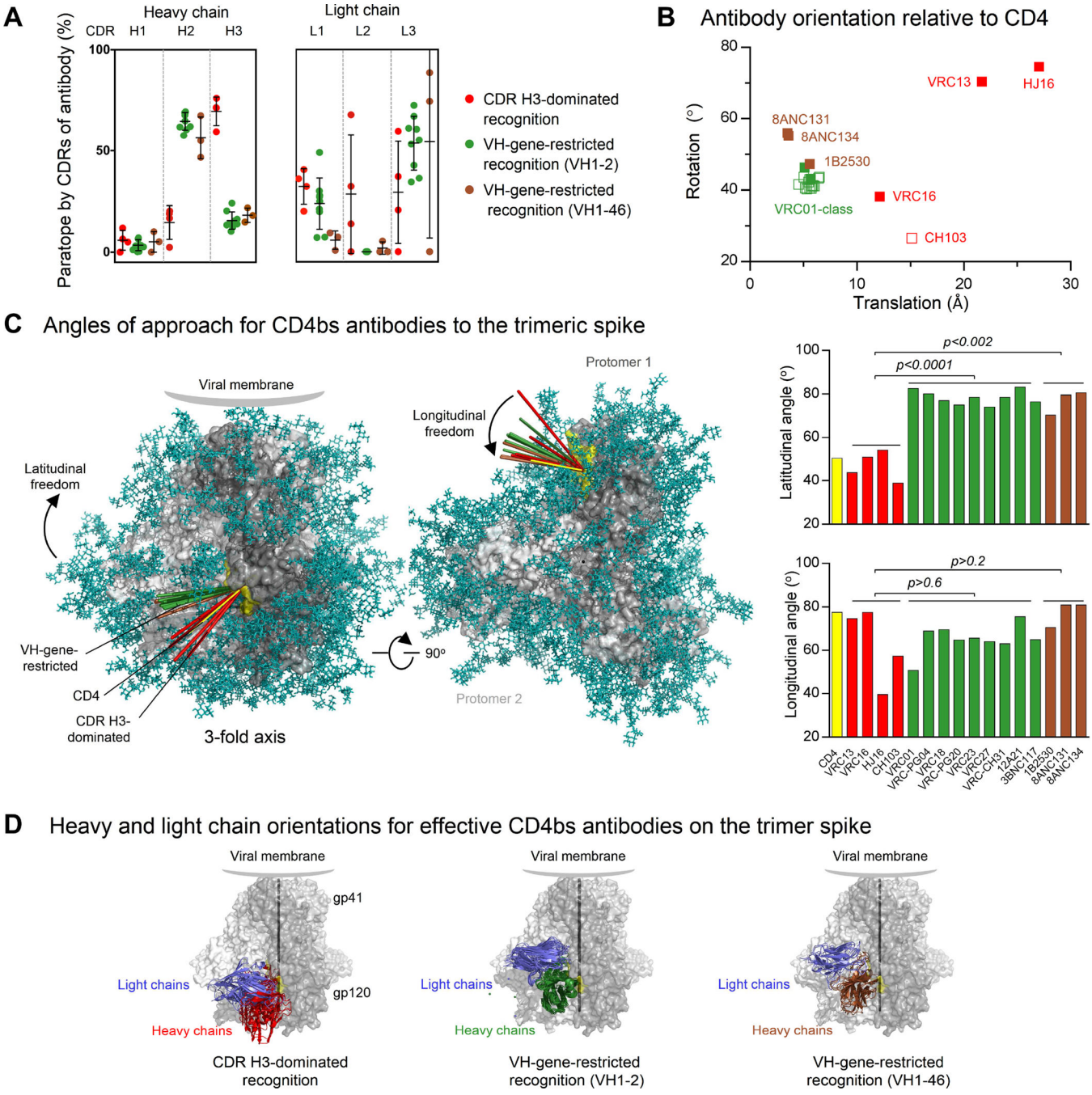

Figure 2. Broadly Neutralizing CD4bs Antibodies Fall into Two Types: CDR H3- Dominated and V_H-Gene-Restricted (VH1-2 or VH1-46)

(A) Percent of surface area buried in the gp120 interface for each CDR of heavy chain (left) and light chain (right). (B) Orientation of heavy-chain component of CD4bs antibody on gp120 relative to CD4. Structures determined here are shown as solid squares. Notably, newly determined structures - 8ANC131, VRC13, VRC16, and HJ16 - have orientations that differ from the previously published VRC01-class and CH103 antibodies. (C) Angles of approach for CD4bs antibodies on the trimer spike in its pre-fusion near-native conformation. Left, the HIV-1 Env trimer is shown as a gray surface with *N*-linked glycans

in teal stick representation. The CD4-binding site on the outer domain of gp120 is represented as a yellow surface; the binding orientation of CD4 (domains 1 and 2) is shown with a yellow line; the binding orientations of CD4bs antibodies are shown with a red line for CDR H3-dominated, green for VH1-2-gene-restricted, and brown for VH1-46-gene-restricted. Right, histogram of explicit angles of approach are provided in the trimer coordinate system shown at left in which a latitudinal angle of 0 coincides with the trimer 3-fold axis. (D) Binding orientation for CDR H3-dominated and VH-gene-restricted CD4bs antibodies. The light chains of antibodies are colored in slate blue and the heavy chains are colored red for CDR H3-dominated antibodies, dark green for VH1-2-gene restricted antibodies, and brown for VH1-46-restricted antibodies. See also Figure S2 and S3, Table S3 and S4.

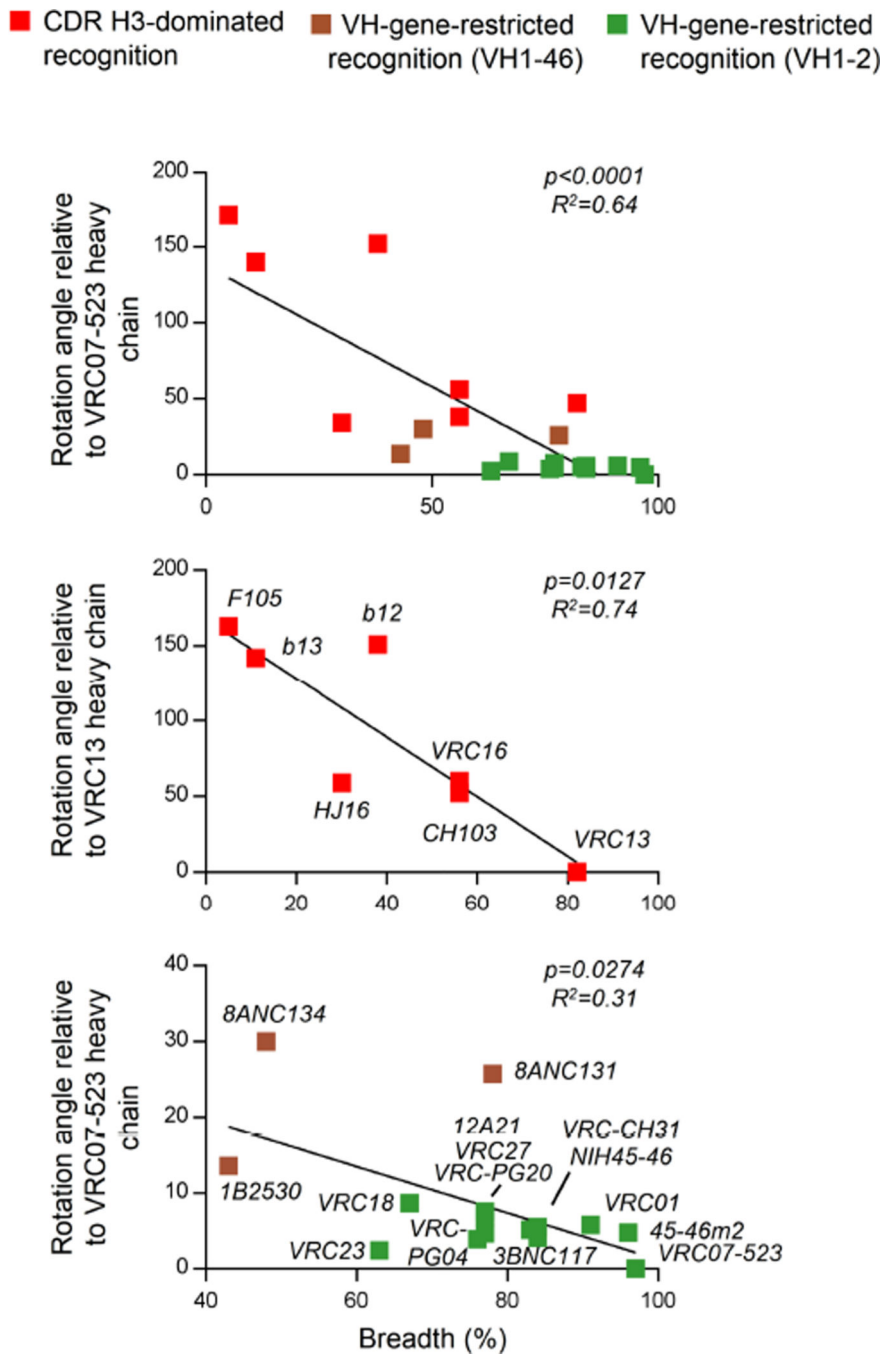

Figure 3. Neutralization Breadth of CD4bs Antibodies Correlates with Angular Difference from the Most Effective Antibodies

Correlation between antibody breadth and the angular difference of the heavy chain relative to the most effective antibodies. Upper panel, all CD4bs antibodies relative to the most effective antibody, VRC07-523; Middle panel, CDR H3-dominated antibodies relative to the most effective CDR H3-dominated antibody, VRC13; Lower panel, VH-gene-restricted antibodies relative to the most effective V_H-gene-restricted antibody, VRC07-523. For clarity, antibodies are only labeled in the middle and lower panels. To determine a common reference frame for calculations of angular difference, antibody-gp120 structures were first

aligned to a common reference frame based on core gp120; to determine angular difference relative to the most effective antibody, a second superposition was performed to align each antibody to the most effective antibody referent; rotation angles determined from this second superposition are shown.

A

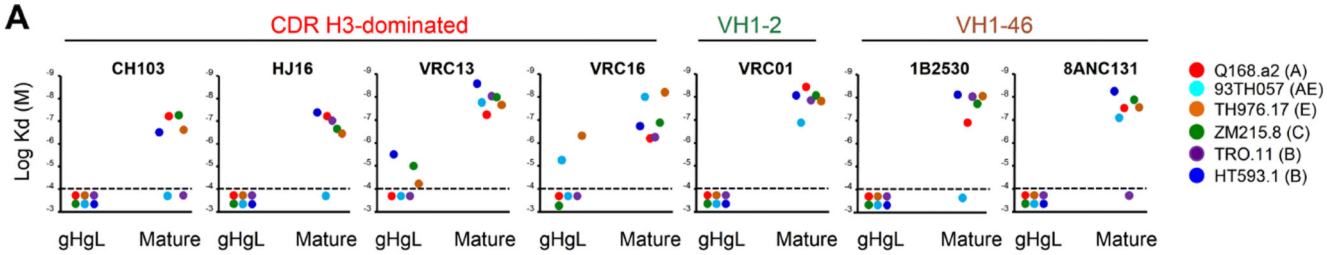

B

Lineage / Antibody	Antibody class (Donor)					
	CDR H3-dominated		VH1-2		VH1-46	
	(44)	(C38)	(45)	(C38)	(RU01)	(RU08)
VRC13.01 / VRC13.02	3671	0	0	0	0	0
VRC16.01 / VRC16.02	0	29	0	0	0	0
VRC01 / VRC03	0	0	5248	15	0	0
VRC18.02 / gVRC$_{dC38}$H3	0	0	829	58	0	0
1NC3 / 1B2530	0	0	0	0	555	0
8ANC131 / 8ANC134	0	0	0	0	270	32

C

Antibody type	Class/donor	Special V_H gene	CDR H3 length	$V_{\kappa/\lambda}$ gene	CDR L3 length	gHgL binding to gp120	Maturation similarities	Sequence signature
CDR H3-dominated	**CH103** Donor: CHAVI505	VH4-59	13	λ3-1	10	Only to autologous	High SHM	
	HJ16 Donor: 242315	VH3-30	19	κ4-1	8	No binding	High SHM	
	VRC13 Donor: 44	VH1-69	21	λ2-14	6	To 50% of heterologous	High SHM	
	VRC16 Donor: C38	VH2-23	20	κ1-39	9	To 33% of heterologous	High SHM	
VH-gene-restricted	**VRC01** Donor: 45, 127/C, C38, CHAVI0219, IAVI23, IAVI57, IAVI74, Z258, RU3	VH1-2	10 to 16	often VK1-33 and VK3-20 (also VK3-15, VI2-14)	5	No binding	Evolutionary similarity in heavy chain	In CDR L3, third position hydrophobic, fourth position E/Q
	8ANC131 Donor: RU1, RU8	VH1-46	16	VK1-47, VI3-11	9 to 11	No binding	Evolutionary similarity in heavy chain	

Figure 4. Characteristics of B Cell Ontogenies for Effective CD4bs Antibodies

(A) Affinities for germline reverted (gHgL) and mature antibodies to six diverse gp120s. Clade of each isolate is shown in parentheses after the strain name. (B) Similarities in heavy chain maturation. Numbers in the table correspond to the number of heavy chain sequences retrieved from heavy chain transcripts determined by NGS of B cells from each donor; retrieval was accomplished by cross-donor phylogenetic analysis with the template antibody from the first column. Gray highlighted areas correspond to matching lineages and classes. The table diagonal represents matching antibodies and donors; when antibodies are found off the diagonal, this indicates similarity in heavy chain maturation. (C) Class characteristics of effective CD4bs antibodies. See also Figure S4 and Table S5.

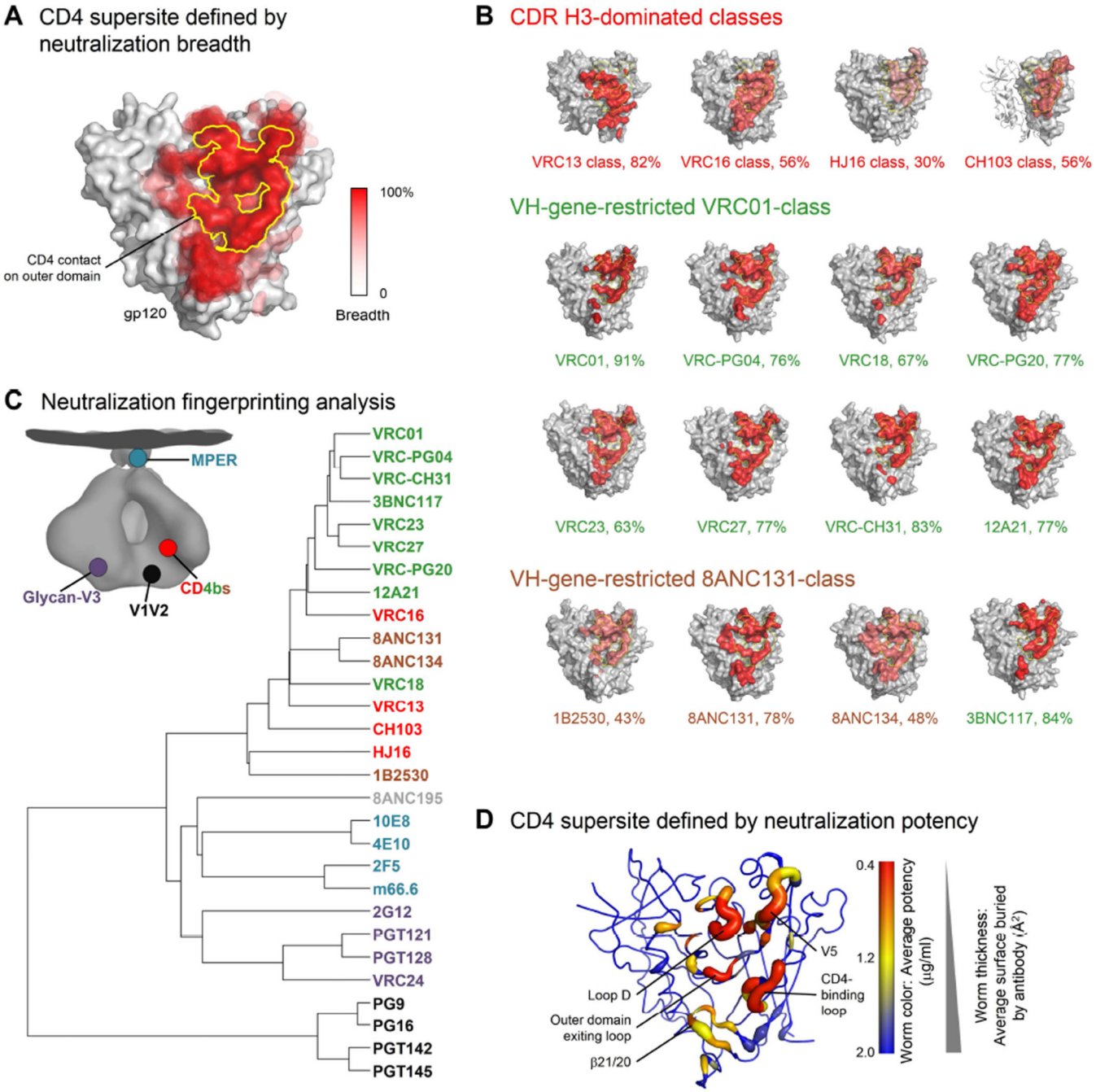

Figure 5. The CD4 Supersite

(A) Antibodies from 14 donors define an immunological supersite of HIV-1 vulnerability. A composite of the breadth-coded epitope surfaces shown in (B) are mapped to the gp120 surface. The yellow outline defines the outer-domain contact of the CD4 receptor. (B) Epitopes of CD4bs antibodies colored by breadth. (C) Dendrogram constructed from similarities in neutralization fingerprint based on serologic analysis with a 178 virus panel; insert shows the HIV-1 viral spike, with membrane at top, with major epitopes labeled; epitope colors correspond to antibody colors in the dendrogram. (D) Potency of CD4-

binding site antibodies mapped to the supersite. The worm representation of HIV-1 gp120 is colored by averaged antibody potency with thickness representing average buried binding surface area of corresponding residues; notably, in addition to the outer domain contact on gp120 for CD4, neighboring regions in the inner domain and on strands β20/21 contribute to the supersite. See also Figure S5.

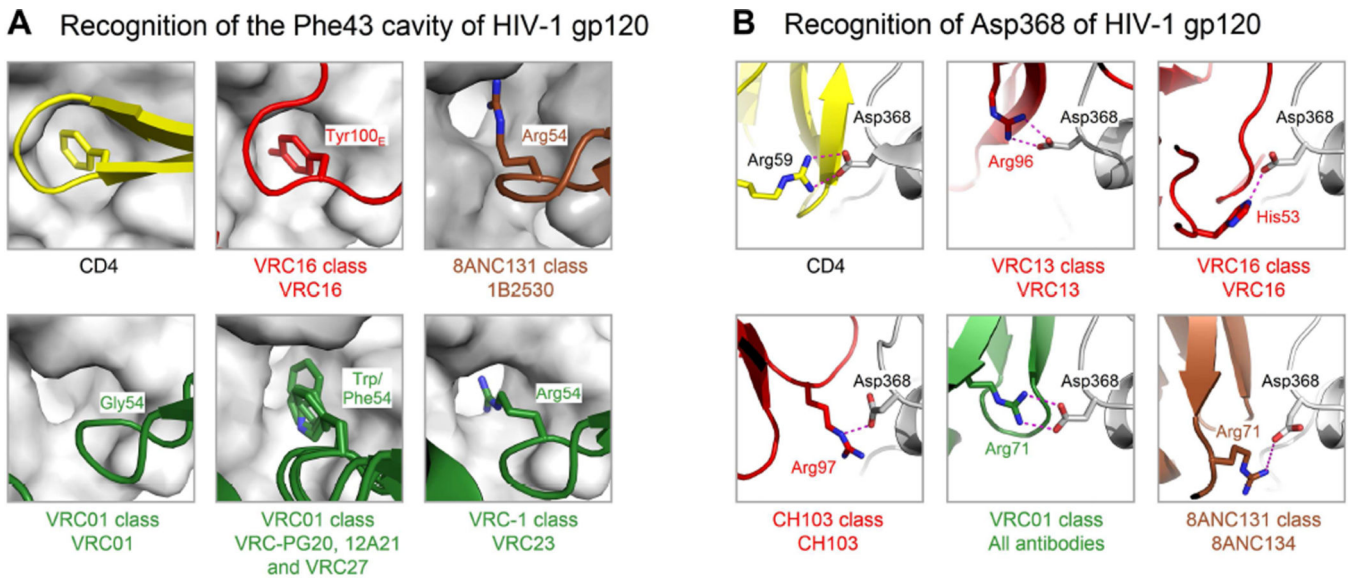

Figure 6. Paratopes of Effective CD4bs Antibodies Are Extremely Diverse

Recognition hotspots of CD4bs antibodies and CD4 are shown with antibodies labeled by class (top line) and representative member (bottom line). (A) CD4bs recognition of Phe43 cavity. Antibody or CD4 are shown in ribbon representation, with the side chain closest to the Phe43 cavity shown in stick representation; gp120 is shown as a gray surface. (B) CD4bs recognition of Asp368 on gp120. Coloring is the same as in (A), but gp120 is shown in ribbon representation, with the Asp368 side chain in stick representation. See also Figure S6 and Table S6.

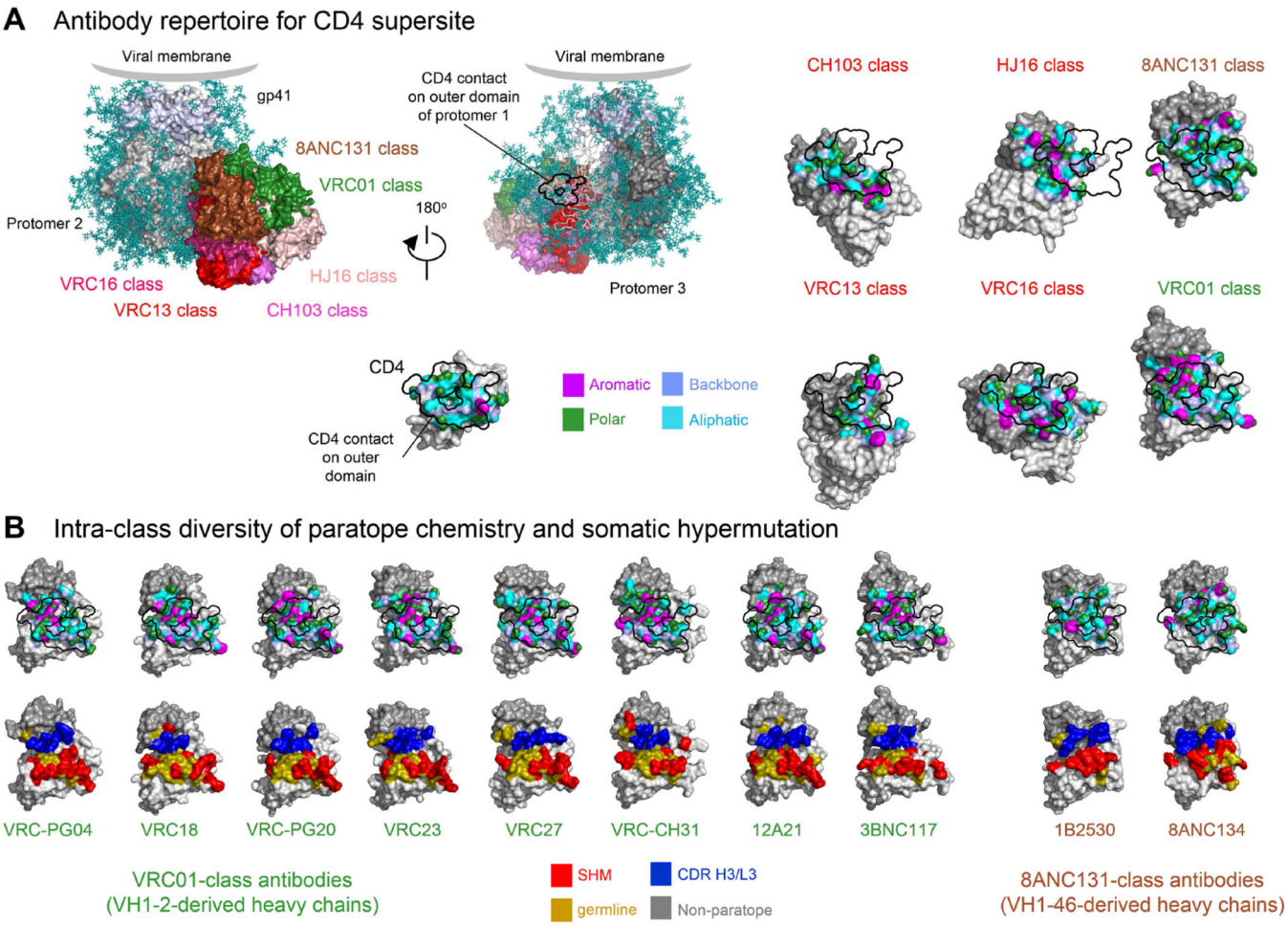

Figure 7. Chemistry of CD4 Supersite Recognition by Effective Neutralizing Antibodies

(A) Chemistry of recognition surfaces is shown for each of the CD4bs antibody classes and CD4. Antibody 8ANC131 is shown for 8ANC131 class; VRC01 is shown for the VRC01 class. Insets show these representative members of each antibody class bound to the CD4 supersite on the HIV-1 Env trimer (gray surface, with *N*-linked glycans shown in teal stick representation). (B) Intra-class comparison of paratope atom type (top row, colored as in key for (A)) and somatic hypermutation (bottom row, with colors defined in key for (B)). See also Figure S7 and Table S7.